

# Experimental and theoretical studies of the decomposition of new imidazole based energetic materials: Model systems

Zijun Yu and Elliot R. Bernstein

Citation: *The Journal of Chemical Physics* **137**, 114303 (2012); doi: 10.1063/1.4752654

View online: <http://dx.doi.org/10.1063/1.4752654>

View Table of Contents: <http://aip.scitation.org/toc/jcp/137/11>

Published by the *American Institute of Physics*

---

---

**COMPLETELY**

**REDESIGNED!**



**PHYSICS  
TODAY**

*Physics Today* Buyer's Guide  
Search with a purpose.

# Experimental and theoretical studies of the decomposition of new imidazole based energetic materials: Model systems

Zijun Yu and Elliot R. Bernstein<sup>a)</sup>

Department of Chemistry, Colorado State University, Fort Collins, Colorado 80523, USA

(Received 18 May 2012; accepted 30 August 2012; published online 18 September 2012)

Decomposition of three imidazole based model energetic systems (2-nitroimidazole, 4-nitroimidazole, and 1-methyl-5-nitroimidazole) is investigated both experimentally and theoretically. The initial decomposition mechanism for these three nitroimidazoles is explored with nanosecond energy resolved spectroscopy, and quantum chemical theory at the complete active space self-consistent field (CASSCF) level. The NO molecule is observed as an initial decomposition product from these three nitroimidazoles subsequent to UV excitation. A unique, excitation wavelength independent dissociation channel is observed for these three nitroimidazoles that generates the NO product with a rotationally cold ( $\sim 50$  K) and a vibrationally mildly hot ( $\sim 800$  K) distribution. Potential energy surface calculations at the CASSCF/6-31G(d) level of theory illustrate that conical intersections play an important and essential role in the decomposition mechanism. Electronically excited  $S_2$  nitroimidazole molecules relax to the  $S_1$  state through the  $(S_2/S_1)_{CI}$  conical intersection, and undergo a nitro-nitrite isomerization to generate the NO product from the  $S_1$  potential energy surface. Nevertheless,  $NO_2$  elimination and nitro-nitrite isomerization are expected to be competitive reaction mechanisms for the decomposition of these molecules on the ground state potential energy surface from the Franck-Condon equilibrium geometry through thermal dissociation. © 2012 American Institute of Physics. [<http://dx.doi.org/10.1063/1.4752654>]

## I. INTRODUCTION

As energetic materials (explosives, propellants, and pyrotechnics) are used extensively both for civil and military applications, high performance and safety have been of primary importance in the development and implementation of new energetic materials for various applications. Imidazole based energetic materials have recently drawn considerable attention due to their high heats of formation, favorable detonation performance, good thermal stabilities, and impact and shock insensitivity.<sup>1-8</sup>

In recent studies, Cho *et al.* reinvestigated the synthesis of 1-methyl-2,4,5-trinitroimidazole, and further characterized its physical properties. Preliminary sensitivity tests reveal that 1-methyl-2,4,5-trinitroimidazole is a promising candidate as an insensitive high explosive, with its explosive performance compared to RDX and its sensitivity between that of RDX and TNT.<sup>1</sup> Heats of formation of a number of energetic species, such as substituted imidazole, 1,2,4-triazole, and tetrazole molecules and ions containing amino, azido, and nitro substituents have been calculated by Dixon's group at the MP2/complete basis set level using isodesmic reactions.<sup>3,4</sup> Based on the DFT method, heats of formation, and molecular stability, detonation performance of nitroimidazole, polynitroimidazole, and their methyl derivatives have been explored. Calculated results disclose that the high performance of imidazole based energetic materials increases with the number of nitro groups for polynitroimidazoles, and their impact sensi-

tivity is directly related to the ratio of the weakest bond to the total energy.<sup>6,7</sup>

Some studies have already been performed on imidazole derivatives, but most of them only focus on either on the macro thermal kinetics to reveal performance, stability, and sensitivity of imidazole derivatives as energetic materials,<sup>3,4,6,7</sup> or on their bioactivity since the imidazole ring is an important constituent of many of biological compounds.<sup>9</sup> To the best of our knowledge, no research has been reported on the unimolecular, isolated molecule decomposition of imidazole based energetic materials. Even though energetic materials are almost always employed as high-density materials, in order to understand their initial decomposition steps and overall mechanism, one must separate and elucidate their intra- and intermolecular behavior and properties. The first step in chemical-to-mechanical energy transformation must involve the breaking of a molecular chemical bond. Even if the condensed, high density phase behavior and mechanism are different from the molecular one, knowing the molecular behavior and the initial bond rupture or weakening for the isolated molecule is an essential step for elucidation of the entire decomposition process. Second, many energetic materials and intermediate species may indeed decompose in gas phase, on a timescale that insures isolation. Initiation of the decomposition reaction can occur by rapid heating, arcs, sparks, shocks, or from a "primary" explosive that begins the process. All of these initiation methods can generate gas phase species whose molecular chemistry can play an important role in the overall mechanism and kinetics of the energetic material decomposition.<sup>10</sup> With regard to photochemical reactions in energetic materials, some very

<sup>a)</sup> Author to whom correspondence should be addressed. Electronic mail: [erb@lamar.colostate.edu](mailto:erb@lamar.colostate.edu).

interesting and germane phenomena can be highlighted: placing certain organic crystals (e.g., lifesavers, sugar, and wintergreen compounds) in a mortar and mechanically grinding them with a pestle, generates light. Emission can be found from  $O^{\pm,0}$ ,  $N^{\pm,0}$ ,  $N_2^{\pm,0}$ ,  $O_2^{\pm,0}$ , and  $C_2^{\pm,0}$ , along with that from the molecules comprising the crystals and fragment radicals. The light is called triboluminescence<sup>11–20</sup> and even laser induced shock waves external to the crystals can generate excited electronic states.<sup>18,21–25</sup> Note that the ionization energy of  $N_2$  itself is over 15.5 eV and this only generates  $N_2^+(X)$ ! How does this happen and from where does all the energy come? Recall that the electrical potential between crystal planes is  $\sim 10^8$  V/cm and, as the crystal fractures, this energy can easily remove electrons from molecules in the crystal, especially at defect and inclusion sites.<sup>26–29</sup> Electrons can be very reactive in initiating chemical decomposition. Shock and compression waves can also generate excited electronic states by excitonic and by HOMO/LUMO gap modulation molecular mechanisms. Core electron excitations have also been suggested as the initial step in condensed phase valence excitation. Additionally, the initiating event in the decomposition of energetic materials can also be a light pulse from a laser. Thus ignition processes involving sparks, shock, slow/rapid heating, lasers, and arcs can all initiate the decomposition reaction of energetic materials by generating excited electronic states.<sup>11–13,16,25,30–35</sup> Investigations of the gas phase, isolated molecule decomposition of these nitroimidazoles following electronic excitation will yield an improved understanding of the initial decomposition mechanisms and dynamics for imidazole based energetic materials.

In this work, we will focus on understanding the decomposition mechanisms and the dynamics of nitroimidazole derivatives (2-nitroimidazole, 4-nitroimidazole, and 1-methyl-5-nitroimidazole, structures shown in Fig. 1) under unimolecular conditions. Nanosecond energy resolved spectroscopy is employed to investigate the excited electronic state decomposition mechanisms and dynamics of isolated gas phase nitroimidazoles. Combined with quantum mechanical calculations (CASSCF), ground and electronic excited state potential energy surfaces (PESs) of these nitroimidazoles are explored in order to generate decomposition mechanisms. Therefore, several detailed insights into the unimolecular decomposition behavior of these nitroimidazoles from their excited electronic states will be discussed in this paper. The present study aims to aid in the design of nitroimidazoles for explosive applications by uncovering their unimolecular decomposition dynamics and kinetics from experiment and theory. This is certainly the first step in the explication of the release of the stored energy in any energetic material, and the

major concern for the synthesis of new and improved “energetic molecules.”<sup>36</sup>

## II. EXPERIMENTAL PROCEDURES

The experimental setup consists of ns laser systems, a supersonic jet expansion pulsed nozzle, and a time-of-flight mass spectrometer chamber, described in detail elsewhere.<sup>37,38</sup> Briefly, for the ns laser experiments, a single pump-probe laser beam at three separate wavelengths (226, 236, and 248 nm) is employed both to initiate dissociation of nitroimidazole molecules and to detect NO following a one-color (1 + 1) resonance enhanced, two photon ionization (R2PI) scheme ( $A^2\Sigma^+(v' = 0) \leftarrow X^2\Pi(v'' = 0,1)$  and  $I \leftarrow A$  transitions) through time of flight mass spectrometry (TOFMS). The three UV laser wavelengths used in the nanosecond laser experiments are generated by a pulsed dye laser, pumped by the second harmonic (532 nm) of a neodymium doped yttrium aluminum garnet laser’s fundamental output (1.064  $\mu\text{m}$ ), in conjunction with a nonlinear wavelength extension system. The typical pulse energy of the UV laser is 50–300  $\mu\text{J}$ /pulse depending on the exact wavelength of interest for a one-color experiment, which gives a laser beam intensity ( $I$ )  $\sim (0.3\text{--}1.8) \times 10^7$  W/cm<sup>2</sup> for a 8 ns pulse duration at a focused beam diameter of 0.5 mm.

Samples (2-nitroimidazole, 4-nitroimidazole and 1-methyl-5-nitroimidazole) are supplied by Dr. Rao Surapaneni and Mr. Reddy Damavarapu (ARL, Picatinny Arsenal, NJ). The isolated gas phase 2-nitroimidazole and 4-nitroimidazole molecules are produced through a combination of matrix assisted laser desorption (MALD) and supersonic jet expansion. The nozzle employed for the sample beam generation is constructed from a Jordan Co. pulsed valve and a laser desorption attachment.<sup>37</sup> Sample drums for matrix desorption are prepared by wrapping a piece of porous filter paper around a clean aluminum drum. A solution of equimolar amounts of sample and matrix (R6G dye) in acetone is uniformly sprayed on the sample drum. An air atomizing spray nozzle (Spraying System Co.) with siphon pressure of 10 psi is used to deposit ablation samples on the filter paper surface. During the spraying, the drum with attached filter paper is rotated and heated with a halogen lamp to make sure that the sample coating is homogeneous and dry. The dried sample drum is then placed in the laser ablation head/nozzle assembly and put into a vacuum chamber. In order to maintain a fresh sample area for each laser ablation shot, a single motor is used to rotate and translate the sample drum simultaneously. Due to its high vapor pressure, the isolated gas phase 1-methyl-5-nitroimidazole cannot be generated by the MALD method; it is vaporized by heating the nozzle and is entrained in the helium expansion gas. These nitroimidazole molecules, desorbed from the drum by laser ablation at 532 nm or produced by heating, are entrained in the flow of helium gas through a  $2 \times 60$  mm channel in the ablation head, and expanded into the vacuum chamber.

The experiment is run at a repetition rate of 10 Hz. The timing sequence for the pulsed nozzle, ablation laser, and ionization laser is controlled by a time delay generator (SRS DG535). The molecular beam is perpendicularly crossed by a

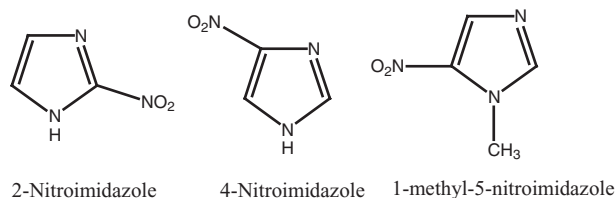


FIG. 1. Molecular structures of three nitroimidazoles.

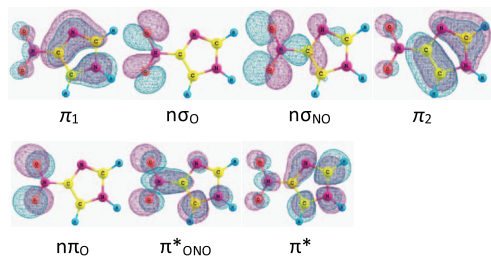


FIG. 2. Orbitals used in the active space (10,7) for CASSCF calculations for the imidazole model molecule 4-nitroimidazole are shown as an example.

UV laser beam that is focused to a spot size of about 0.5 mm at the ionization region of a time-of-flight mass spectrometer. A background pressure of  $2 \times 10^{-6}$  Torr is maintained in the vacuum chamber during the experiment. Ion signals are detected by a microchannel plate detector. Signals are recorded and processed on a personal computer using a boxcar averager (SRS SR 250) and an analog-to-digital conversion card (Analog Devices RTI-800).

### III. COMPUTATIONAL METHODS

All geometry optimizations relevant to decomposition of excited electronic states of nitroimidazoles are executed at the CASSCF/6-31G(d) level of theory within the GAUSSIAN 09 program.<sup>39–45</sup> No symmetry restrictions are applied during the calculations. To explore the excited state PESs, the active space comprises 10 electrons distributed in 7 orbitals, denoted as CASSCF(10,7). Orbitals used in the active space are two  $\pi$ -bonding orbitals of the five-member ring  $\pi_1$  and  $\pi_2$ , one NO nonbonding orbital  $\pi_{NO}$ , one  $\pi$ -nonbonding orbital  $\pi_{NO}$ , one  $\sigma$  nonbonding orbital  $\pi_{NO}$ , one delocalized ONO  $\pi$ -antibonding orbital  $\pi_{ONO}^*$ , and one  $\pi$ -antibonding orbital of the five-member ring  $\pi^*$ . These orbitals are illustrated in Figure 2. The geometries of conical intersections are optimized with state averaging over the  $S_0$  and  $S_1$  states or over  $S_1$  and  $S_2$  with equal weights. Transition state (TS) structures are characterized by analytical frequency calculations. Equilibrium geometry calculations are conducted taking the total charge as neutral and the spin multiplicity as 1 (see supplementary material<sup>62</sup>).

### IV. EXPERIMENTAL RESULTS AND DISCUSSION

Three nitroimidazoles (2-nitroimidazole, 4-nitroimidazole, and 1-methyl-5-nitroimidazole) have been studied at three excitation wavelengths (226, 236, and 248 nm). The parent molecules are excited to an upper vibronic state by absorption of a single UV photon. They decompose into products through specific decomposition pathways. The NO product channel has been detected here as the decomposition pathway of these nitroimidazoles. The NO product is probed using a one color (1 + 1) R2PI detection scheme through TOFMS. Three excitation wavelengths chosen for this work also correspond to the (0–0), (0–1), and (0–2) vibronic bands of the  $A^2\Sigma^+ \leftarrow X^2\Pi$  electronic transition of the NO product. By scanning the nanosecond laser excitation wavelength, a (1 + 1) R2PI rotationally resolved spectrum of the NO product from different parent

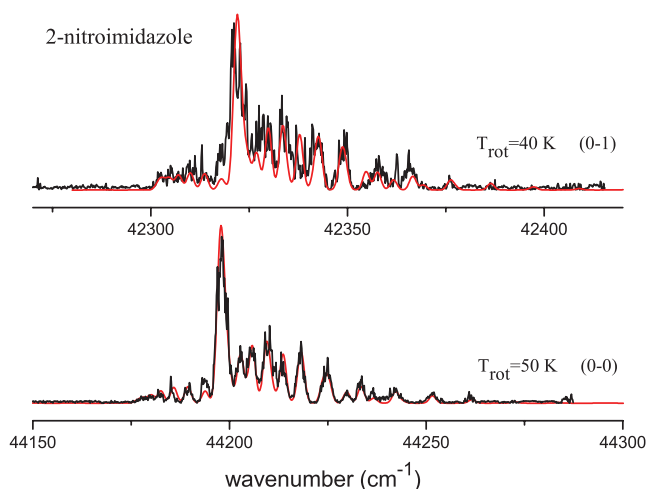


FIG. 3. One color (1 + 1) R2PI spectra of the vibronic transitions  $A^2\Sigma^+(v' = 0) \leftarrow X^2\Pi(v'' = 0,1)$  of the NO product from the decomposition of electronically excited 2-nitroimidazole molecule (model system). Rotational temperature simulations (red) with a Boltzmann population distribution show that these two observed vibrational levels of ground electronic state NO have cold rotational temperatures of 40–50 K. The vibrational temperature of the NO product from 2-nitroimidazole is estimated to be  $\sim 800$  K.

molecules is obtained. The parent molecules have continuous absorption in these wavelength regions.

(1 + 1) R2PI spectra of the two vibronic transitions,  $A^2\Sigma^+(v' = 0) \leftarrow X^2\Pi(v'' = 0,1)$  of the NO product generated by the decomposition of the electronically excited 2-nitroimidazole, 4-nitroimidazole, and 1-methyl-5-nitroimidazole molecules are shown in Figs. 3–5. The most intense feature in each spectrum of NO can be assigned as the ( $Q_{11} + P_{12}$ ) band head of each vibronic band, and the less intense features within each spectrum are due to other rovibronic transitions.<sup>46,47</sup> Two vibronic transitions  $A^2\Sigma^+(v' = 0) \leftarrow X^2\Pi(v'' = 0,1)$  of the NO product have been observed from the decomposition of electronically excited 2-nitroimidazole as shown in Fig. 3. Spectral simulations based on Boltzmann population distributions for the two vibronic transitions produce similar rotational temperatures of 40–50 K. The vibrational temperature of the NO product from 2-nitroimidazole can also be obtained by simulating the relative intensities among the observed vibronic bands using a Boltzmann population distribution analysis and Franck-Condon factors. By comparing the experimental data with simulations at different vibrational temperatures, the vibrational temperature of the NO product from 2-nitroimidazole is estimated to be  $\sim 800$  K. With regard to 4-nitroimidazole, two vibronic transitions  $A^2\Sigma^+(v' = 0) \leftarrow X^2\Pi(v'' = 0,1)$  of the NO product have also been observed from the decomposition of the electronically excited 4-nitroimidazole, as shown in Fig. 4. Rotational temperatures for the two vibronic transitions obtained by simulations based on Boltzmann population distributions are 15 K and 60 K, respectively. The vibrational temperature of the NO product from 4-nitroimidazole is estimated to be  $\sim 900$  K, by using Boltzmann population distribution analysis and Franck-Condon factors. At this point, 2-nitroimidazole and 4-nitroimidazole show similar results for the decomposition

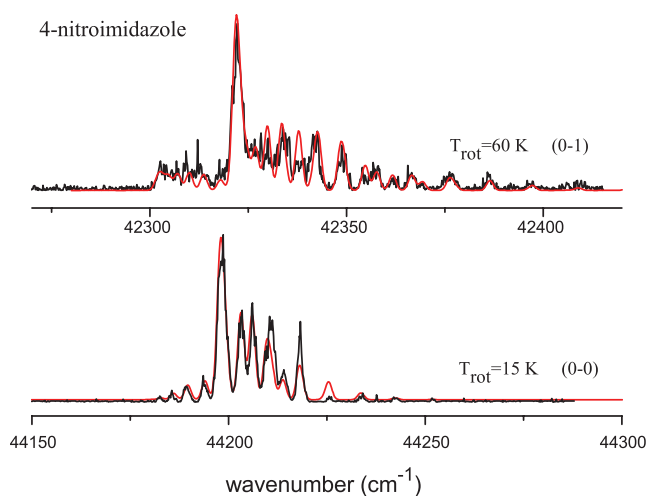


FIG. 4. One color (1 + 1) R2PI spectra of the vibronic transitions  $A^2\Sigma^+(v' = 0) \leftarrow X^2\Pi(v'' = 0,1)$  of the NO product from the decomposition of electronically excited 4-nitroimidazole molecule (model system). Rotational temperature simulations (red) with a Boltzmann population distribution show that these two observed vibrational levels of ground electronic state NO have cold rotational temperatures of 15–60 K. The vibrational temperature of the NO product from 4-nitroimidazole is estimated to be  $\sim 900$  K.

process of the electronically excited, isolated gas phase molecules. They both generate rotationally cold and vibrationally mildly hot distributions for the product NO, no matter where the  $\text{NO}_2$  group is located on the ring. Only one vibronic transition,  $A^2\Sigma^+(v' = 0) \leftarrow X^2\Pi(v'' = 0)$ , for the NO product is observed from the decomposition of electronically excited 1-methyl-5-nitroimidazole, as shown in Fig. 5: the rotational temperature of the NO product for this  $A^2\Sigma^+(v' = 0) \leftarrow X^2\Pi(v'' = 0)$  transition is about 10 K. Even though the 1-methyl-5-nitroimidazole also gives a rotationally cold distribution for its NO product, as is found for 2-nitroimidazole and 4-nitroimidazole, it generates a quite different vibrational temperature for NO in its decomposition dynamical process. Both rotational and vibrational temperatures are quite low for the NO product from 1-methyl-5-nitroimidazole: is this related to the  $\text{NO}_2$  group position on the ring or is it due to the presence of the methyl group? We will discuss this issue in Sec. V.

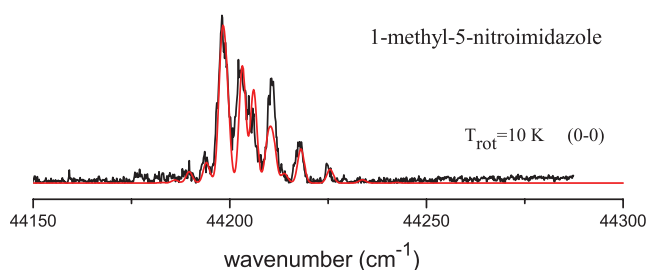


FIG. 5. One color (1 + 1) R2PI spectra of the vibronic transitions  $A^2\Sigma^+(v' = 0) \leftarrow X^2\Pi(v'' = 0)$  of the NO product from the decomposition of electronically excited 1-methyl-5-nitroimidazole molecule (model system). Rotational temperature simulations (red) with a Boltzmann population distribution show that the observed vibrational level of the ground electronic state has a cold rotational temperature of 10 K.

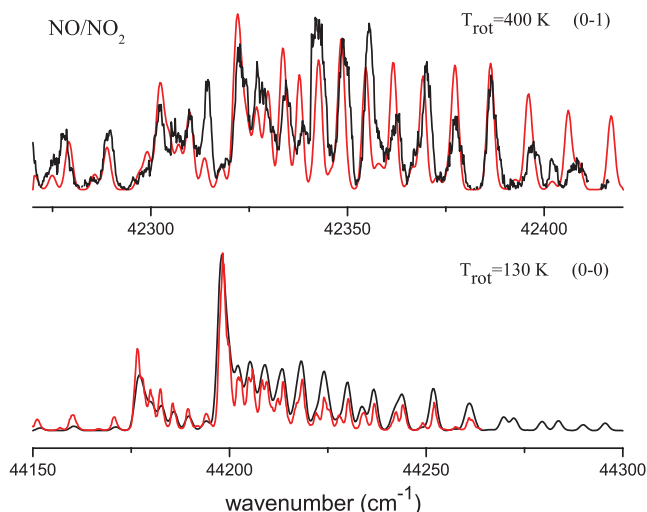


FIG. 6. One color (1 + 1) R2PI spectra of the vibronic transitions  $A^2\Sigma^+(v' = 0) \leftarrow X^2\Pi(v'' = 0,1)$  of the NO product from the decomposition of electronically excited  $\text{NO}_2$ . Rotational temperature is estimated to be 130 K and 400 K for the two vibronic transitions, respectively.

As discussed in our previous research,<sup>48–50</sup>  $\text{NO}_2$  elimination is a possible dissociation channel for nitro-containing model and energetic molecules. Thus, comparison of the above decomposition results with those for the decomposition of electronically excited  $\text{NO}_2$  gas phase molecule is necessary. Figure 6 presents the one color (1 + 1) R2PI spectra of the vibronic transitions  $A^2\Sigma^+(v' = 0) \leftarrow X^2\Pi(v'' = 0,1)$  of the NO product from the decomposition of electronically excited  $\text{NO}_2$ .  $\text{NO}_2$  (0.02%) gas in He has been used in this experiment. Based on a Boltzmann population distribution, the simulated vibronic spectra show a rotational temperature for the NO product from expansion cooled  $\text{NO}_2$  gas is about 130 K for the vibronic transition  $A^2\Sigma^+(v' = 0) \leftarrow X^2\Pi(v'' = 0)$ . The rotational temperature for the NO product for the vibronic transition  $A^2\Sigma^+(v' = 0) \leftarrow X^2\Pi(v'' = 1)$  from  $\text{NO}_2$  is much higher,  $\sim 400$  K. These results mean that if  $\text{NO}_2$  loss were the major reaction channel for decomposition of electronically excited imidazole model species,  $\text{NO}_2$  would subsequently dissociate to NO, in the wavelength range used in our experiments, and thus NO from  $\text{NO}_2$  produced by imidazole model systems should present similar or hotter rotational distributions compared to those from expansion cooled  $\text{NO}_2$  gas. NO from photolysis of nitroimidazoles is, however, rotationally colder than that from expansion cooled  $\text{NO}_2$  gas: this indicates that  $\text{NO}_2$  cannot be the major reaction channel in the decomposition of electronically excited nitroimidazoles. The discussion above also excludes the possibility that  $\text{NO}_2$  is generated in the MALD process and is the precursor for the NO production in our experiment. Thus, the MALD technique is a good method to place easily fragmented, fragile molecules in the gas phase without fragmentation.

With regard to the HONO reaction channel, we have determined in previous work<sup>48,49,51</sup> that HONO elimination in all X- $\text{NO}_2$  system is less than 5% of the NO elimination following the nitro-nitrite isomerization. For nitroimidazoles, HONO elimination is even less likely than for RDX,

DMNA, etc., due to the stiffness of the five-membered aromatic ring. Therefore, NO elimination after nitro-nitrite isomerization should be the major reaction channel for the UV decomposition of nitroimidazoles. In Sec. V, we will explain how NO elimination after nitro-nitrite isomerization becomes the major reaction channel from the theoretical perspective.

So, what we learn from the experiments is the following: (1) NO is the first initial decomposition product from electronically excited nitroimidazoles; (2) the final transition state for NO release does not place a large torque on the exiting NO; and (3) the decomposition probably occurs on an excited electronic state surface because the NO product is not highly vibrationally excited. The next step in the analysis of the decomposition behavior of nitroimidazoles following electronic excitation is to generate a mechanism consistent with these products and internal energy distribution facts: we do this based on quantum mechanical theory and calculations.

## V. THEORETICAL RESULTS AND DISCUSSION

According to previous studies,<sup>48,49,51–54</sup> the major differences found among various experimental results for both thermal (ground state,  $S_0$ ) and excited electronic state ( $S_1$ ) initiated decomposition of nitro-containing model and energetic molecules primarily concern two mechanisms:  $\text{NO}_2$  elimination and nitro-nitrite isomerization. Therefore, the theoretical exploration of these two channels will be explored below in order to judge which of them is energetically more favorable. These results and understandings are necessary and essential for providing new insight into the overall decomposition mechanisms and dynamics of nitroimidazole model molecules.

### A. Ground electronic state decomposition

To compare the two decomposition channels,  $\text{NO}_2$  elimination and nitro-nitrite isomerization followed by NO elimination, energy barriers on the ground state PES, calculated at the MP2/6-31G(p,d) and CASSCF(10,7)/6-31G(d) levels, are listed in Table I. Calculated results at the MP2/6-31G(p,d) level are almost in agreement with those at the CASSCF(10,7)/6-31G(d) level for the ground PES: this is a very encouraging result. The calculations show that the energy barrier (about 80 kcal/mol) needed to perform the C- $\text{NO}_2$  bond dissociation is comparable to that of the nitro-nitrite isomerization for three nitroimidazole model molecules. Thus both  $\text{NO}_2$  elimination and nitro-nitrite isomerization chan-

nels are expected to play a role in the overall thermal decomposition mechanisms and dynamics for these nitroimidazole model molecules on the ground state PES. The branching ratio between these two channels will depend on many factors, e.g., enthalpy and entropy of the reaction, electronically nonadiabatic transitions, etc. This discovery is quite different from nonaromatic, nitramine model molecules (such as, DMNA, etc.),<sup>48</sup> or energetic molecules (such as, RDX, PETN, etc.),<sup>50,55</sup> which we studied before. DMNA needs about 40 kcal/mol energy to break N- $\text{NO}_2$  bond or 94 kcal/mol energy to activate nitro-nitrite isomerization.<sup>48</sup> About 41 kcal/mol energy can break the N- $\text{NO}_2$  bond in RDX, and the activation barrier for nitro-nitrite isomerization is about 92 kcal/mol.<sup>55</sup> PETN needs only 35 kcal/mol to initiate  $\text{NO}_2$  elimination, and 60 kcal/mol activation energy to complete nitro-nitrite isomerization.<sup>50</sup> Even though calculational methods are different for DMNA, RDX, and PETN, comparing these calculated results, the whole reaction trend for the three samples is consistent. At low temperature thermolysis or decomposition on the ground state PES,  $\text{NO}_2$  elimination is expected to be the major decomposition channel for DMNA, RDX, and PETN: this has also been demonstrated by other researchers.<sup>56–59</sup> Nitroimidazole model molecules, however, represent different dynamics and kinetics on the ground state PES based on our calculations: (1) even though we do not simulate the dynamics or kinetics of NO/ $\text{NO}_2$  elimination on the ground state PES, we can suggest that  $\text{NO}_2$  elimination and nitro-nitrite isomerization will compete with each other for the decomposition mechanism, because the barriers for the two processes are comparable; and (2) due to the imidazole ring, nitroimidazole model molecules have stronger C-N bonds than other model or energetic molecules, such as, DMNA, RDX, and PETN. Nitroimidazole model molecules have better stability, so it is expected that nitroimidazole energetic molecules will also have better stability and lower impact/shock sensitivity than other energetic molecules, like RDX and PETN, even if the molecule does not stay on the ground state PES during the initiation (shock, thermal, etc.) process, this respective stability/bond energy comparative relation can still obtain.

### B. Decomposition following electronic state excitation

With regard to decomposition of excited electronic state nitroimidazole model molecules, a comparison between the computed vertical and the experimental excitation energies has been made employing the CASSCF method,

TABLE I. Barriers (kcal/mol) of  $\text{NO}_2$  elimination and nitro-nitrite isomerization on the ground state for three nitroimidazole model molecules.

	MP2/6-31G(p,d)		CAS(10,7)/6-31G(d)	
	$\text{NO}_2$ elimination	Nitro-nitrite isomerization	$\text{NO}_2$ elimination	Nitro-nitrite isomerization
2-nitroimidazole	79.1	78.4	81.9	77.4
4-nitroimidazole	86.0	83.2	77.3	90.7
1-methyl-5-nitroimidazole	86.7	89.8	78.6	93.7

TABLE II. Vertical excitation energy (in eV) for three nitroimidazole model molecules, calculated at the CASSCF(10,7)/6-31G(d).

Compound	$S_1(n \rightarrow \pi^*)$	$S_2(n \rightarrow \pi^*)$	$S_3(\pi \rightarrow \pi^*)$
2-nitroimidazole	3.79	4.71	5.61
4-nitroimidazole	3.92	4.70	6.30
1-methyl-5-nitroimidazole	3.97	4.85	5.42

in order to assess which excited states are relevant to our experimental observations. The vertical excitation energies for 2-nitroimidazole, 4-nitroimidazole, and 1-methyl-5-nitroimidazole, calculated at the CASSCF(10,7)/6-31G(d) optimized Frank-Condon geometry (ground state minimum) are listed in Table II: the calculated vertical excitation energies of the  $S_1$  states for 2-nitroimidazole, 4-nitroimidazole, and 1-methyl-5-nitroimidazole are 3.79, 3.92, and 3.97 eV, respectively; the calculated vertical excitation energies of the  $S_2$  states for these three nitroimidazole molecules are 4.71, 4.70 and 4.85 eV, respectively; and the calculated vertical excitation energies of the  $S_3$  states for these three nitroimidazole molecules are 5.61, 6.30, and 5.42 eV, respectively. Since no experimental values for vertical excitation energies of nitroimidazole molecules have been published so far, the experimental UV-Vis absorption of 4-nitroimidazole has been executed to compare to the calculated results. As shown in Fig. 7, the UV-Vis absorption spectrum of 4-nitroimidazole in cyclohexane has three maxima at 311 nm (3.98 eV), 287 nm (4.32 eV), and 203 nm (6.11 eV), which are almost in agreement with the calculated values 3.92, 4.70, and 6.30 eV. This comparison reveals that the CASSCF method with a (10,7) active space gives a reasonable treatment of the relevant excited states. Comparison of the excitation energies (5.49 eV at 226 nm, 5.25 eV at 236 nm, and 5.00 eV at 248 nm) used in this work with the calculated vertical excitation energies (listed in Table II) for the  $S_2$  and  $S_3$  excited states of nitroimidazole model molecules, the three nitroimidazole model

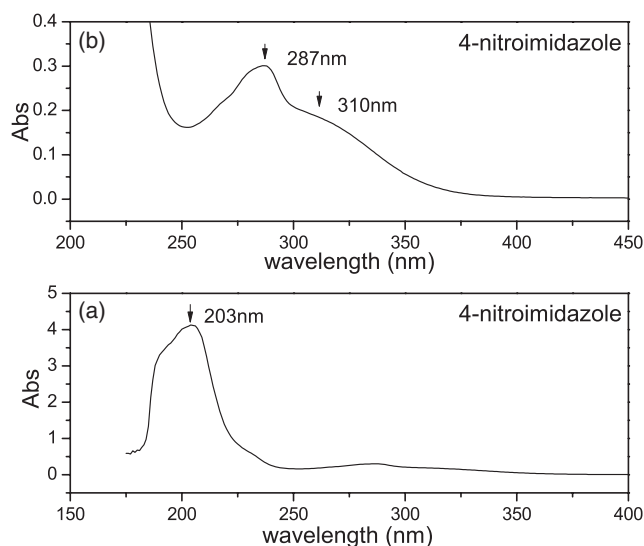


FIG. 7. The UV-Vis absorption spectrum of 4-nitroimidazole in cyclohexane.

molecules are mostly excited to their  $S_2$  excited states by these three excitation wavelengths.

The CASSCF calculations also reveal that the three nitroimidazole model molecules have similar excitation transition no matter where the  $\text{NO}_2$  group is located on the ring: the three lowest lying excited states for these molecules are  $(n, \pi^*)$ ,  $(n, \pi^*)$ , and  $(\pi, \pi^*)$  states, which correspond to  $S_1$ ,  $S_2$ , and  $S_3$  excited electronic states, respectively. The electronic transitions to the  $S_1$  ( $n, \pi^*$ ) and  $S_2$  ( $n, \pi^*$ ) states of the three nitroimidazoles (that is, excitation from the nonbonding orbital  $n\sigma_{\text{NO}}$  or the nonbonding orbital  $n\sigma_{\text{O}}$  of oxygen in  $\text{NO}_2$  to the  $\text{ONO}$   $\pi$ -antibonding orbital  $\pi_{\text{ONO}^*}$ ) are the same as those for DMNA and  $\text{CH}_3\text{NO}_2$ .<sup>48,49</sup> But the electronic transitions to the  $S_3$  ( $\pi, \pi^*$ ) states of the three nitroimidazoles (i.e., electron excitation from the  $\pi$ -bonding orbitals of the imidazole ring to the  $\text{ONO}$   $\pi$ -antibonding orbital  $\pi_{\text{ONO}^*}$ ) are quite different from those of DMNA and  $\text{CH}_3\text{NO}_2$  (electron excitation from the  $\pi$ -nonbonding orbital  $n\pi_{\text{O}}$  of oxygen in  $\text{NO}_2$  to the  $\text{ONO}$   $\pi$ -antibonding orbital  $\pi_{\text{ONO}^*}$ ) due to the presence of the aromatic imidazole ring.

### 1. 2-nitroimidazole

In order to account for our experimental results more completely,  $S_0$ ,  $S_1$ , and  $S_2$  electronic surfaces of the three nitroimidazole model molecules have been explored theoretically. Schematic one-dimensional projections of the multi-dimensional PESs ( $S_0$ ,  $S_1$ , and  $S_2$ ) of 2-nitroimidazole with locations and structures of different critical points is plotted in Fig. 8. The relative CASSCF energies of the critical points (minimum, conical intersection/CI, transition state/TS) for excited states ( $S_2$ ,  $S_1$ ) and the ground state ( $S_0$ ) PES of 2-nitroimidazole, with respect to the energy of ground state FC geometry, are presented in the figure (the calculated energies have not been corrected for zero point energy). The optimized ground state geometry “FC geometry” of 2-nitroimidazole is a planar structure. Two essential and mechanism dominating conical intersections are located on the potential energy surfaces: “ $(S_1/S_0)_{\text{CI}}$ ” represents the conical intersection between the ground electronic state  $S_0$  and the first electronic excited state  $S_1$  (the computed energy gap between  $S_0$  and  $S_1$  at  $(S_1/S_0)_{\text{CI}}$  conical intersection is about  $125 \text{ cm}^{-1}$ ); “ $(S_2/S_1)_{\text{CI}}$ ” represents the conical intersection between the second excited electronic state  $S_2$  and the first electronic excited state  $S_1$  (the computed energy gap between  $S_2$  and  $S_1$  at the  $(S_2/S_1)_{\text{CI}}$  conical intersection is about  $65 \text{ cm}^{-1}$ ). “ $S_{0,\text{nitrite}}$ ” and “ $S_{1,\text{nitrite}}$ ” are nitrite structures of 2-nitroimidazole after nitro-nitrite isomerization on  $S_0$  and  $S_1$ , respectively. “ $S_{0,\text{TS,NO-elimin}}$ ” and “ $S_{1,\text{TS,NO-elimin}}$ ” are transition states for NO elimination from the nitrite structure of 2-nitroimidazole on  $S_0$  and  $S_1$ ; the arrows in the structure of the transition states show the reaction coordinate of the imaginary frequency.

From the explored potential energy surfaces in Fig. 8, two possible decomposition channels for 2-nitroimidazole following electronic excitation to  $S_2$  along different relevant nuclear coordinates can be found. One potential decomposition pathway for the 2-nitroimidazole parent molecule would be to move along the  $S_2$  surface, transition to the  $S_1$

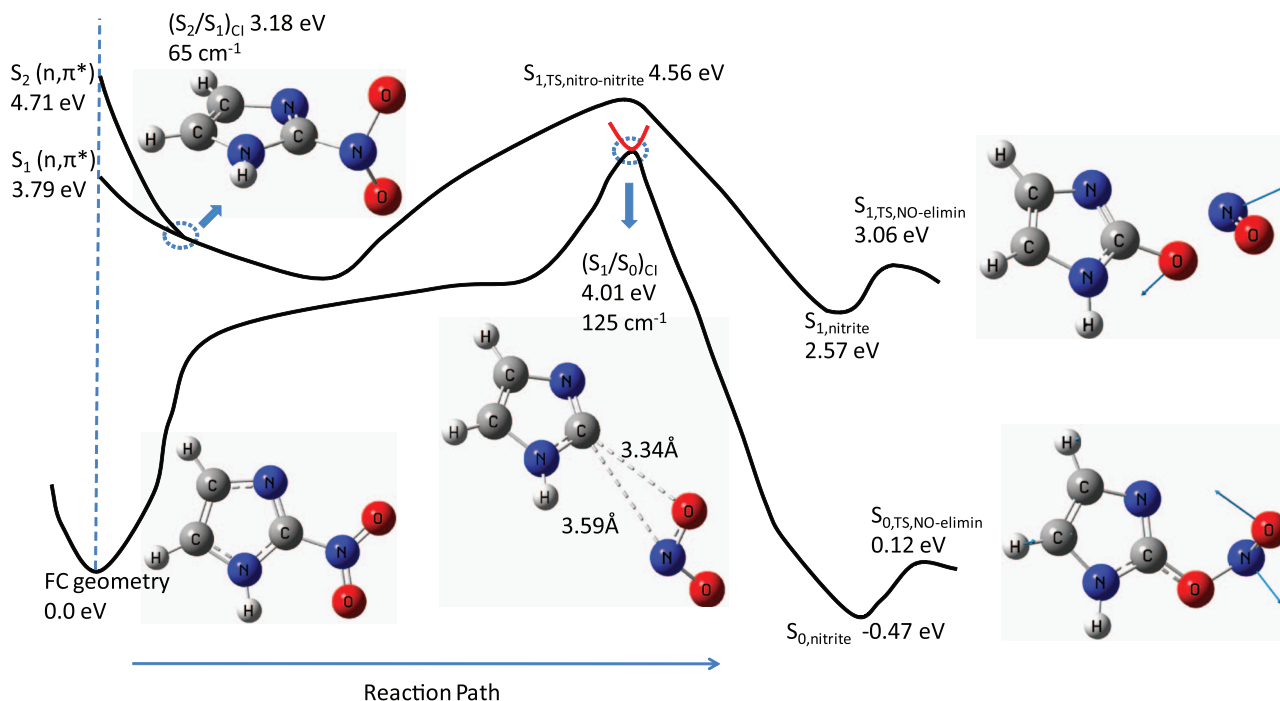


FIG. 8. A schematic one-dimensional projection of the multi-dimensional potential energy surfaces of 2-nitroimidazole computed at the CASSCF(10,7)/6-31G(d) level of theory. The solid red line, which represents the  $S_1$  electronic excited state, is generated by a different reaction coordinate. “FC geometry,” which is a planar structure, is the optimized minimum energy structure of 2-nitroimidazole on  $S_0$  state. “ $(S_1/S_0)_{CI}$ ” represents the conical intersection between the ground and first excited electronic states. The adiabatic energy gap at this point is  $\sim 125 \text{ cm}^{-1}$ . “ $(S_2/S_1)_{CI}$ ” represents the conical intersection between the second and first excited electronic states. The adiabatic energy gap at this point is  $\sim 65 \text{ cm}^{-1}$ . “ $S_{1,TS,nitro-nitrite}$ ” is the transition state of the nitro-nitrite isomerization on the  $S_1$  state. “ $S_{0,nitrite}$ ” and “ $S_{1,nitrite}$ ” are nitrite structures of 2-nitroimidazole after nitro-nitrite isomerization on  $S_0$  and  $S_1$ , respectively. “ $S_{0,TS,NO-elimin}$ ” and “ $S_{1,TS,NO-elimin}$ ” are transition states for NO elimination from the nitrite structure of 2-nitroimidazole on  $S_0$  and  $S_1$ , respectively. The arrows in the structure of the transition states show the reaction coordinate of the imaginary frequency.

surface by crossing through the  $(S_2/S_1)_{CI}$  conical intersection, and remain on the  $S_1$  surface. The molecule must then surmount the  $S_{1,TS,nitro-nitrite}$  transition state to initiate the nitro-nitrite isomerization on the  $S_1$  surface. For subsequent NO elimination on the  $S_1$  PES, 2-nitroimidazole would need to surmount the  $S_{1,TS,NO-elimin}$  transition state subsequent to the nitro-nitrite isomerization. The energy barrier to subsequent NO loss is about 0.49 eV with respect to the  $S_{1,nitrite}$  local minimum. The other possible decomposition pathway is that the 2-nitroimidazole molecule, which decays to the  $S_1$  surface through the  $(S_2/S_1)_{CI}$  conical intersection, will continue to descend to the  $S_0$  surface through the  $(S_1/S_0)_{CI}$  conical intersection and then reach a nitro-nitrite isomer along the descent path on the  $S_0$  surface. After overcoming a small barrier (0.59 eV), NO product would be generated on the  $S_0$  state.

The first dissociation channel,  $S_1$  generation of NO, is chosen to be the most probable reaction channel for 2-nitroimidazole. Two reasons can be cited for this behavior or mechanism. First, on theoretical grounds, even though a weak (adiabatic energy gap  $\sim 125 \text{ cm}^{-1}$ ) conical intersection  $(S_1/S_0)_{CI}$  between the  $S_1$  electronic excited state and the  $S_0$  ground state has been found for 2-nitroimidazole, the actual nuclear coordinate for this intersection is complicated and involves a number of different normal modes, due to the large change in geometry between the  $(S_1/S_0)_{CI}$  conical intersection structure and the  $S_0$  structure (see Fig. 8). Second, we have also performed experiments on nitroimidazole energetic molecules, such as 1,4-dinitroimidazole, 2,4-

dinitroimidazole, and 1-methyl-2,4-dinitroimidazole; the vibrational temperatures obtained for NO from these energetic molecules is about 1600 K. Based on our previous studies of the decomposition of energetic molecules,<sup>38,50,55,60,61</sup> the molecules typically descend to the ground state through a series of conical intersections and generate rotationally cold and vibrationally hot distributions for the NO product. The vibrational temperature of NO products, generated from model molecules, usually is much colder than that of energetic molecules. So on experimental grounds, if the model molecule 2-nitroimidazole relaxes to the ground state through conical intersections and dissociates on the ground state PES, it should have sufficient energy to excite the NO vibration to a level similar to that found for the energetic molecules (1,4-dinitroimidazole, 2,4-dinitroimidazole, and 1-methyl-2,4-dinitroimidazole). Therefore, from the above discussion, the decomposition mechanism that 2-nitroimidazole parent molecule, excited to the  $S_2$  electronic excited state, undergoes is as follows: (1) the molecule excited to the  $S_2$  electronic state relaxes to  $S_1$  electronic excited state through the  $(S_2/S_1)_{CI}$  conical intersection; (2) the molecule surmounts the transition state barrier on  $S_1$  to form the nitro-nitrite isomer which finally gives birth to NO product; and (3) the imaginary frequency of vibration for the NO elimination transition state on the  $S_1$  surface of 2-nitroimidazole shows only a small component of torque on the eliminated NO. Thus  $S_1$  dissociation for NO generates a rotationally cold and vibrationally warm NO product, in agreement with our experimental

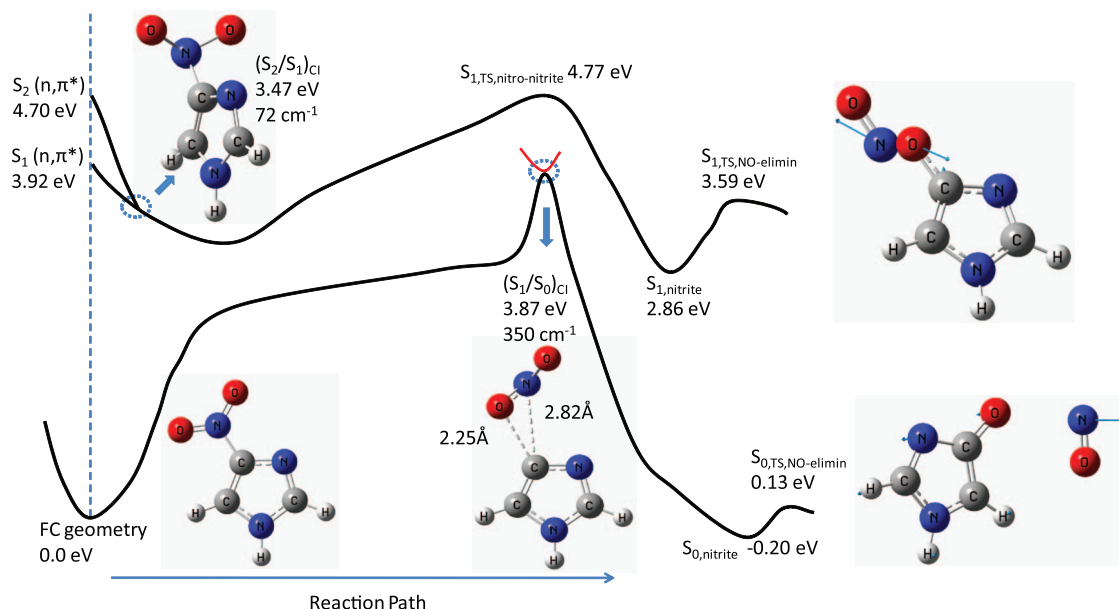


FIG. 9. A schematic one-dimensional projection of the multidimensional potential energy surfaces of 4-nitroimidazole computed at the CASSCF(10,7)/6-31G(d) level of theory. The solid red line, which represents the  $S_1$  electronic excited state, is generated by a different reaction coordinate. “FC geometry,” which is a planar structure, is the optimized minimum energy structure of 2-nitroimidazole on the  $S_0$  state. “ $(S_1/S_0)_{CI}$ ” represents the conical intersection between the ground and first excited electronic states. The adiabatic energy gap at this point is  $\sim 350\text{ cm}^{-1}$ . “ $(S_2/S_1)_{CI}$ ” represents the conical intersection between the second and first excited electronic states. The adiabatic energy gap at this point is  $\sim 72\text{ cm}^{-1}$ . “ $S_{1,TS,nitro-nitrite}$ ” is the transition state of the nitro-nitrite isomerization on the  $S_1$  state. “ $S_{0,nitrite}$ ” and “ $S_{1,nitrite}$ ” are nitrite structures of 4-nitroimidazole after nitro-nitrite isomerization on  $S_0$  and  $S_1$ , respectively. “ $S_{0,TS,NO-elimin}$ ” and “ $S_{1,TS,NO-elimin}$ ” are transition states for NO elimination from the nitrite structure of 4-nitroimidazole on  $S_0$  and  $S_1$ . The arrows in the structure of the transition states show the reaction coordinate of the imaginary frequency.

results (rotational temperature 40–50 K, vibrational temperature 800 K).

## 2. 4-nitroimidazole

The schematic one-dimensional projection of the multidimensional potential energy surfaces ( $S_0$ ,  $S_1$ , and  $S_2$ ) of 4-nitroimidazole with locations and structures of different critical points is shown in Fig. 9. The relative CASSCF (adiabatic state) energies of the critical points (minimum, conical intersection/CI, transition state/TS) on excited states ( $S_2$ ,  $S_1$ ) and the ground state ( $S_0$ ) PESs of 4-nitroimidazole with respect to the energy of ground state FC geometry are also present (the calculated energies have not been corrected for zero point energy). The optimized ground state geometry “FC geometry” of 4-nitroimidazole is a planar structure like 2-nitroimidazole. Two important conical intersections “ $(S_1/S_0)_{CI}$ ” and “ $(S_2/S_1)_{CI}$ ” are also found on the potential energy surfaces. The computed energy gap for  $(S_1/S_0)_{CI}$  and  $(S_2/S_1)_{CI}$  conical intersections is about 350 and  $72\text{ cm}^{-1}$ , respectively. The whole potential energy surfaces are similar to those of 2-nitroimidazole, therefore it is expected that 4-nitroimidazole has a similar decomposition mechanism to that of 2-nitroimidazole. The 4-nitroimidazole parent molecule excited to the  $S_2$  electronic state by absorbing one photon, relaxes to the  $S_1$  electronic excited state through the  $(S_2/S_1)_{CI}$  conical intersection and then surmounts the nitro-nitrite isomerization barrier on the  $S_1$  state to form the nitro-nitrite isomer which finally generates NO product. The arrows in the structure of the transition states “ $S_{1,TS,NO-elimin}$ ” in Fig. 9 show the reaction coordinate of the imaginary frequency, which re-

veals that there is not a large component of torque on the eliminated NO. Thus, this transition state is expected to produce a rotationally cold NO product in agreement with our experimental results. Following vertical excitation of the parent molecule to its higher vibronic manifold of the  $S_2$  surface, and then undergoing rapid nonadiabatic internal conversion from  $S_2$  to  $S_1$  through the  $(S_2/S_1)_{CI}$  conical intersection, and thereafter from the nitro-nitrite isomerization to NO elimination, the molecule can store enough electronic excitation energy in its vibrational degrees of freedom on the  $S_1$  surface pathway to excite the vibration of the final NO moiety. Based on the above discussion, rotationally cold and vibrationally warm distributions of NO product from the  $S_1$  surface is reasonable and in accord with our experimental results (rotational temperature 15–60 K, vibrational temperature 900 K).

## 3. 1-methyl-5-nitroimidazole

The schematic one-dimensional projection of the multidimensional potential energy surfaces ( $S_0$ ,  $S_1$ , and  $S_2$ ) for 1-methyl-5-nitroimidazole, with locations and structures of different critical points, is shown in Fig. 10. The relative CASSCF energies of the critical points (minimum, conical intersection/CI, transition state/TS) on excited states ( $S_2$ ,  $S_1$ ) and the ground state ( $S_0$ ) PESs of 1-methyl-5-nitroimidazole with respect to the energy of ground state FC geometry are also presented (the calculated energies have not been corrected for zero point energy). The optimized ground state geometry “FC geometry” of 1-methyl-5-nitroimidazole has the  $\text{NO}_2$  group and the imidazole ring at the same plane. Two important conical intersections “ $(S_1/S_0)_{CI}$ ” and “ $(S_2/S_1)_{CI}$ ”

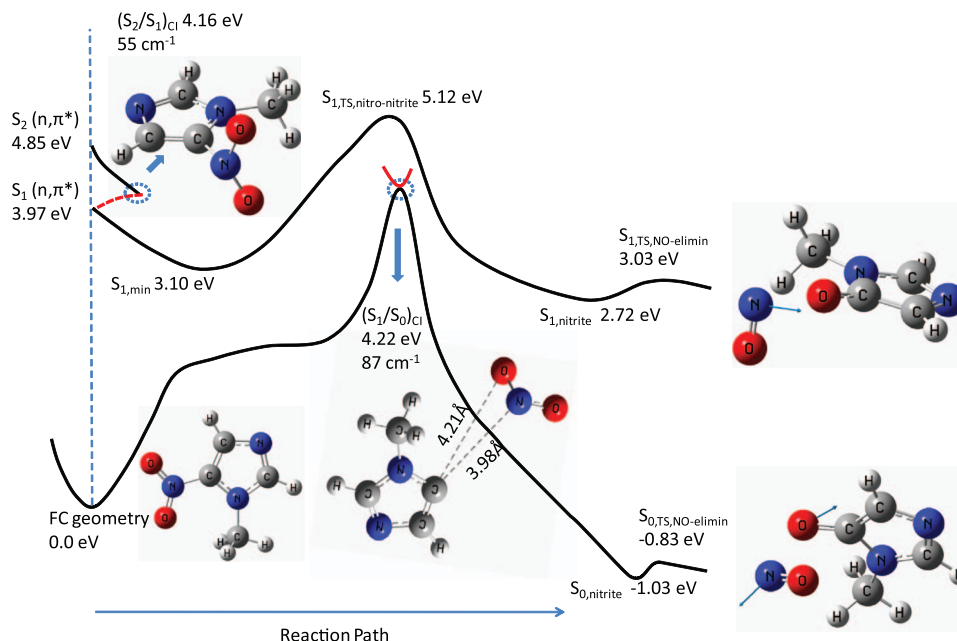


FIG. 10. A schematic one-dimensional projection of the multidimensional potential energy surfaces of 1-methyl-5-nitroimidazole computed at the CASSCF(10,7)/6-31G(d) level of theory. The solid red line, which represents the  $S_1$  electronic excited state, is generated by a different reaction coordinate. “FC geometry” is the optimized minimum energy structure of 2-nitroimidazole on  $S_0$  state. “ $(S_1/S_0)_{CI}$ ” represents the conical intersection between the ground and first excited electronic states. The adiabatic energy gap at this point is  $\sim 87 \text{ cm}^{-1}$ . “ $(S_2/S_1)_{CI}$ ” represents the conical intersection between the second and first excited electronic states. The adiabatic energy gap at this point is  $\sim 55 \text{ cm}^{-1}$ . “ $S_{1,TS,nitro-nitrite}$ ” is the transition state of the nitro-nitrite isomerization on the  $S_1$  state. “ $S_{0,nitrite}$ ” and “ $S_{1,nitrite}$ ” are nitrite structures of 1-methyl-5-nitroimidazole after nitro-nitrite isomerization on  $S_0$  and  $S_1$ , respectively. “ $S_{0,TS,NO-elimin}$ ” and “ $S_{1,TS,NO-elimin}$ ” are transition states for NO elimination from the nitrite structure of 1-methyl-5-nitroimidazole on  $S_0$  and  $S_1$ , respectively. The arrows in the structure of the transition states show the reaction coordinate of the imaginary frequency.

are also found on the potential energy surfaces. The computed energy gaps for  $(S_1/S_0)_{CI}$  and  $(S_2/S_1)_{CI}$  conical intersections are about  $87$  and  $55 \text{ cm}^{-1}$ , respectively. Even though only one vibronic transition,  $A^2\Sigma^+(\nu' = 0) \leftarrow X^2\Pi(\nu'' = 0)$ , of the NO product has been observed for 1-methyl-5-nitroimidazole in our experiments, we still propose that the 1-methyl-5-nitroimidazole molecule has a similar decomposition mechanism as that suggested for 2-nitroimidazole and 4-nitroimidazole. Parent molecules excited to the  $S_2$  state descend to the  $S_1$  state through the  $(S_2/S_1)_{CI}$  conical intersection, and generate a NO molecule following a nitro-nitrite isomerization on the  $S_1$  potential energy surface. This common mechanism is favored for all three nitroimidazole molecules for three reasons. First, the whole potential energy surfaces and critical points found based on CASSCF calculation for 1-methyl-5-nitroimidazole are similar to those of 2-nitroimidazole and 4-nitroimidazole. The related excited states in our experiments and calculations for these three nitroimidazole model molecules are the same:  $S_1(n, \pi^*)$ , and  $S_2(n, \pi^*)$ , excitation from the nonbonding orbital  $n\sigma_{NO}$  or the nonbonding orbital  $n\sigma_O$  on oxygen of  $NO_2$  to the  $ONO \pi$ -antibonding orbital  $\pi_{ONO^*}$ . Thus 1-methyl-5-nitroimidazole, 2-nitroimidazole, and 4-nitroimidazole should have similar dynamical decompositions mechanisms despite the presence of the methyl group. Second, the methyl group has many low frequency vibrational modes that can resonantly absorb energy in the decomposition process and thereby reduce the vibrational energy of the final NO product. We estimate that the vibrational temperature of 1-methyl-5-nitroimidazole should be less than  $\sim 500 \text{ K}$  for the absence of the 0-1 NO tran-

sition. Third, the 1-methyl-5-nitroimidazole parent molecule vapor is produced by heating the nozzle in a flow of helium gas in this experiment: due to its high vapor pressure, the MALD vaporization approach, used for 2-nitroimidazole and 4-nitroimidazole, cannot be employed for 1-methyl-5-nitroimidazole. Heating may not generate as much imidazole vapor as does the MALD method, and this could also contribute to the weak or missing signal for the  $A^2\Sigma^+(\nu' = 0) \leftarrow X^2\Pi(\nu'' = 1)$  transition of the NO product from 1-methyl-5-nitroimidazole. The signal/noise ratio for the spectra of Figs. 3–5 should be compared.

Based on above discussion, the decomposition mechanism for the three nitroimidazole model molecules can be given as follows: the parent molecule, excited to the  $S_2$  electronic excited state by absorbing a photon, relaxes to the  $S_1$  electronic state through the  $(S_2/S_1)_{CI}$  conical intersection, and then surmounts the barrier to form a nitro-nitrite isomer on the  $S_1$  state, which finally generates rotationally cold and vibrationally mildly hot distributions for the NO product. Our previous studies on nitro-containing model molecules<sup>48,51</sup> show that either they dissociate on the excited state PES and NO, as the major product, has a rotationally hot and vibrationally cold distribution, such as occurs for DMNA,<sup>48</sup> or they dissociate on the ground state PES and NO, which comes from the precursor  $NO_2$ , has a rotationally hot and vibrationally mildly hot distribution, such as occurs for  $CH_3NO_2$  and isopropyl nitrate.<sup>51</sup> Nitroimidazole model molecules present an additional phenomenon for nitro-containing model systems. In 226 nm photolysis, the related electronic state transition for  $CH_3NO_2$  and isopropyl nitrate is a  $\pi^* \leftarrow \pi$  transition;

however, for nitroimidazole model molecules and DMNA, the related electronic state transition is  $\pi^* \leftarrow n$ . This may be the reason why  $\text{CH}_3\text{NO}_2$  and isopropylnitrate behave so differently from the other model molecules. Nitroimidazole model molecules and DMNA have similar low lying excited states ( $\pi^* \leftarrow n$  transition); nonetheless, they demonstrate different dissociation mechanisms. The imidazole aromatic ring is the key. Based on the above discussion, we can conclude that the imidazole model molecules still dissociate on their excited state PESs as most nitro-containing model molecules. The apparent difference of the mechanism of decomposition between imidazole based model molecules and imidazole based energetic molecules lies in the accessibility of the  $(S_1/S_0)_{\text{CI}}$ : for energetic molecules, this conical intersection is taken to  $S_0$  and decomposition follows a nitro-nitrite isomerization, which yields product NO with cold rotational and hot vibrational distributions; for model molecules, this conical intersection is not taken and the molecule decomposes on the excited state surface. For the energetic molecules, the fragmented NO is, thereby, a much hotter, more reactive molecular radical species with regard to both translations and vibrations. In a word, decomposition of electronically excited  $\text{NO}_2$  containing energetic materials occurs to yield NO product from their highly vibrationally excited  $S_0$  states after following a series of conical intersections to their ground electronic states. These molecules give rotationally cold and vibrationally hot distributions of NO. Conical intersections play a crucial role in the initial decomposition for electronically excited energetic materials. The relaxation pathways through a series of conical intersections leave the energetic molecule on a part of the ground state surface that is typically inaccessible from the ground state equilibrium position. Decomposition of electronically excited nitro-containing model molecules, however, occurs from their excited electronic states. The rotational and vibrational temperatures of the NO product from these molecules are related to the molecular structure of the final transition state for the dissociation.

Besides, the three nitroimidazole model molecules have similar PESs and decomposition mechanisms, which mean that the position of  $\text{NO}_2$  group does not have an important effect on their dissociation dynamics. But all three nitroimidazole model molecules are of the C- $\text{NO}_2$  form. A question worthy of further study is: how do N- $\text{NO}_2$  nitroimidazoles behave under the same set of investigations.

## VI. CONCLUSIONS

The decomposition of three nitroimidazole model molecules following electronic excitation has been investigated via nanosecond energy resolved spectroscopy. These nitroimidazoles (2-nitroimidazole, 4-nitroimidazole, and 1-methyl-5-nitroimidazole) generate NO as an initial decomposition product at the nanosecond laser excitation wavelengths (248, 236, 226 nm), with vibrationally warm and rotationally cold distributions of the NO product, which are independent of excitation wavelengths. Based on the experimental observations and CASSCF calculations, we conclude that the decomposition of electronically excited nitroimidazole model molecules occurs on the  $S_1$  electronic excited state PES. Par-

ent molecules excited to the  $S_2$  state descend to the  $S_1$  state through the  $(S_2/S_1)_{\text{CI}}$  conical intersection, and generate a NO molecule following a nitro-nitrite isomerization on the  $S_1$  potential energy surface.

Based on previous studies of energetic and model molecules, one may conclude: (1) decomposition of electronically excited nitro-containing model molecules occurs from their excited electronic states; (2) the rotational and vibrational temperatures of the NO product are related to the molecular structure of the final transition state for the dissociation, even though the relevant low lying excited states arise from the same  $\pi^* \leftarrow n$  transitions for most nitro-containing model molecules; (3) conical intersections also take part in the decomposition process for model molecules; (4) different positions of the  $\text{NO}_2$  group on the ring do not change the dissociation dynamics or mechanisms of nitroimidazole model molecules; and (5) both  $\text{NO}_2$  elimination and nitro-nitrite isomerization are available for the decomposition of nitroimidazoles on their ground state PESs for thermal,  $S_0$  dissociation, unlike other nitro-containing energetic and model molecules for which the lower energy decomposition path on  $S_0$  is generation of  $\text{NO}_2$ .

## ACKNOWLEDGMENTS

This study is supported by a grant from the U.S. Army Research Office (ARO, FA9550-10-1-0454) and in part by the U.S. National Science Foundation (NSF) through the XSEDE supercomputer resources provided by NCSA under Grant No. TG-CHE110083. We thank Dr. Rao Surapaneni and Mr. Reddy Damavarapu (ARL, Picatinny Arsenal, NJ) for supplying the samples used in this research.

- <sup>1</sup>J. R. Cho, K. J. Kim, S. G. Cho, and J. K. Kim, *J. Heterocycl. Chem.* **39**, 141 (2002).
- <sup>2</sup>B. M. Rice, S. Sahu, and F. J. Owens, *J. Mol. Struct.: THEOCHEM* **583**, 69 (2002).
- <sup>3</sup>K. E. Gutowski, R. D. Rogers, and D. A. Dixon, *J. Phys. Chem. A* **110**, 11890 (2006).
- <sup>4</sup>K. E. Gutowski, R. D. Rogers, and D. A. Dixon, *J. Phys. Chem. B* **111**, 4788 (2007).
- <sup>5</sup>H. S. Jadhav, M. B. Talawar, R. Sivabalan, D. D. Dhavale, S. N. Asthana, and V. N. Krishnamurthy, *J. Hazard. Mater.* **143**, 192 (2007).
- <sup>6</sup>X. F. Su, X. L. Cheng, C. M. Meng, and X. L. Yuan, *J. Hazard. Mater.* **161**, 551 (2009).
- <sup>7</sup>X. H. Li, R. Z. Zhang, and X. Z. Zhang, *J. Hazard. Mater.* **183**, 622 (2010).
- <sup>8</sup>P. Ravi, G. M. Gore, S. P. Tewari, and A. K. Sikder, *J. Mol. Model.* **18**, 597 (2012).
- <sup>9</sup>J. C. Lee, J. T. Laydon, P. C. McDonnell, T. F. Gallagher, S. Kumar, D. Green, D. McNulty, M. J. Blumenthal, J. R. Heys, S. W. Landvatter, J. E. Strickler, M. M. McLaughlin, I. R. Siemens, S. M. Fisher, G. P. Livi, J. R. White, J. L. Adams, and P. R. Young, *Nature (London)* **372**, 739 (1994).
- <sup>10</sup>R. W. Shaw, T. B. Brill, and D. L. Thompson, *Overviews of Recent research on Energetic Materials* (World Scientific, Hackensack, NJ, 2005).
- <sup>11</sup>H. M. Windawi, S. P. Varma, C. B. Cooper, and F. Williams, *J. Appl. Phys.* **47**, 3418 (1976).
- <sup>12</sup>J. Schanda, B. Baron, and F. Williams, *J. Lumin.* **9**, 338 (1974).
- <sup>13</sup>S. P. Varma and F. Williams, *J. Chem. Phys.* **59**, 912 (1973).
- <sup>14</sup>F. Williams, *Adv. Chem. Phys.* **21**, 289 (1971).
- <sup>15</sup>J. Sharma, J. W. Forbes, C. S. Coffey, and T. P. Liddiard, *J. Phys. Chem.* **91**, 5139 (1987).
- <sup>16</sup>J. Sharma, B. C. Beard, and M. Chaykovsky, *J. Phys. Chem.* **95**, 1209 (1991).
- <sup>17</sup>Z. A. Dreger, Y. A. Gruzdkov, Y. M. Gupta, and J. J. Dick, *J. Phys. Chem. B* **106**, 247 (2001).

- <sup>18</sup>Y. Tsuboi, T. Seto, and N. Kitamura, *J. Phys. Chem. B* **107**, 7547 (2003).
- <sup>19</sup>B. P. Aduiev, E. D. Aluker, M. M. Kuklja, A. B. Kunz, and E. H. Younk, *J. Lumin.* **91**, 41 (2000).
- <sup>20</sup>M. M. Kuklja, S. N. Rashkeev, and F. J. Zerilli, *AIP Conf. Proc.* **706**, 363 (2004).
- <sup>21</sup>E. J. Reed, J. D. Joannopoulos, and L. E. Fried, *Phys. Rev. B* **62**, 16500 (2000).
- <sup>22</sup>M. Manaa, L. Fried, and E. Reed, *J. Comput.-Aided Mater. Des* **10**, 75 (2003).
- <sup>23</sup>M. R. Manaa and L. E. Fried, *J. Phys. Chem. A* **103**, 9349 (1999).
- <sup>24</sup>M. M. Kuklja, E. V. Stefanovich, and A. B. Kunz, *J. Chem. Phys.* **112**, 3417 (2000).
- <sup>25</sup>M. M. Kuklja, B. P. Aduiev, E. D. Aluker, V. I. Krasheninina, A. G. Krechetov, and A. Y. Mitrofanov, *J. Appl. Phys.* **89**, 4156 (2001).
- <sup>26</sup>M. M. Kuklja and A. B. Kunz, *J. Phys. Chem. Solids* **61**, 35 (2000).
- <sup>27</sup>C. M. Tarver, *AIP Conf. Proc.* **1426**, 227 (2012).
- <sup>28</sup>A. B. Kunz and D. R. Beck, *Phys. Rev. B* **36**, 7580 (1987).
- <sup>29</sup>D. G. Tasker, R. D. Dick, and W. H. Wilson, *AIP Conf. Proc.* **429**, 591 (1998).
- <sup>30</sup>A. Bhattacharya, Y. Guo, and E. R. Bernstein, *Acc. Chem. Res.* **43**, 1476 (2010).
- <sup>31</sup>J. Sharma and B. C. Beard, *Mater. Res. Soc. Symp. Proc.* **296**, 189 (1993).
- <sup>32</sup>J. J. Gilman, *Mat. Res. Soc. Symp. Proc.* **453**, 227 (1997).
- <sup>33</sup>B. P. Aduiev, E. D. Aluker, G. M. Belokurov, Y. A. Zakharov, and A. G. Krechetov, *J. Exp. Theor. Phys.* **89**, 906 (1999).
- <sup>34</sup>A. B. Kunz, M. M. Kuklja, T. R. Botcher, and T. P. Russell, *Thermochim. Acta* **384**, 279 (2002).
- <sup>35</sup>R. B. Hall and F. Williams, *J. Chem. Phys.* **58**, 1036 (1973).
- <sup>36</sup>Even though the term “energetic molecule” is not a completely accurate descriptor, it is a jargon in this field. Thus we will still use this phrase in this report. In this sense, an “energetic molecule” is one that, in a pure crystalline form, will be able to detonate or release its stored chemical energy successfully in a short period of time.
- <sup>37</sup>H. S. Im and E. R. Bernstein, *J. Chem. Phys.* **113**, 7911 (2000).
- <sup>38</sup>Y. Q. Guo, M. Greenfield, and E. R. Bernstein, *J. Chem. Phys.* **122**, 244310 (2005).
- <sup>39</sup>M. J. Frisch, G. W. Trucks, H. B. Schlegel *et al.*, GAUSSIAN 09, Revision A.1; Gaussian, Inc., Wallingford, CT, 2009.
- <sup>40</sup>I. J. Palmer, I. N. Ragazos, F. Bernardi, M. Olivucci, and M. A. Robb, *J. Am. Chem. Soc.* **115**, 673 (1993).
- <sup>41</sup>D. Asturiol, B. Lasorne, G. A. Worth, M. A. Robb, and L. Blancafort, *Phys. Chem. Chem. Phys.* **12**, 4949 (2010).
- <sup>42</sup>D. Peláez, J. F. Arenas, J. C. Otero, and J. Soto, *J. Org. Chem.* **72**, 4741 (2007).
- <sup>43</sup>J. Soto, J. F. Arenas, J. C. Otero, and D. Peláez, *J. Phys. Chem. A* **110**, 8221 (2006).
- <sup>44</sup>K. Fukui, *Acc. Chem. Res.* **14**, 363 (1981).
- <sup>45</sup>H. P. Hratchian and H. B. Schlegel, *J. Chem. Theory Comput.* **1**, 61 (2004).
- <sup>46</sup>C. J. S. M. Simpson, P. T. Griffiths, H. L. Wallaart, and M. Towrie, *Chem. Phys. Lett.* **263**, 19 (1996).
- <sup>47</sup>G. Herzberg, *Molecular Spectra and Molecular Structure: Spectra of Diatomic Molecules* (Van Nostrand, New York, 1950).
- <sup>48</sup>A. Bhattacharya, Y. Q. Guo, and E. R. Bernstein, *J. Phys. Chem. A* **113**, 811 (2009).
- <sup>49</sup>Y. Q. Guo, A. Bhattacharya, and E. R. Bernstein, *J. Phys. Chem. A* **113**, 85 (2008).
- <sup>50</sup>Z. J. Yu and E. R. Bernstein, *J. Chem. Phys.* **135**, 154305 (2011).
- <sup>51</sup>A. Bhattacharya, Y. Guo, and E. R. Bernstein, *J. Chem. Phys.* **136**, 024321 (2012).
- <sup>52</sup>Y. Q. Guo, M. Greenfield, A. Bhattacharya, and E. R. Bernstein, *J. Chem. Phys.* **127**, 154301 (2007).
- <sup>53</sup>L. J. Butler, D. Krajnovich, Y. T. Lee, G. S. Ondrey, and R. Bersohn, *J. Chem. Phys.* **79**(4), 1708 (1983).
- <sup>54</sup>J. M. Flournoy, *J. Chem. Phys.* **36**, 1106 (1962).
- <sup>55</sup>A. Bhattacharya and E. R. Bernstein, *J. Phys. Chem. A* **115**, 4135 (2011).
- <sup>56</sup>S. A. Lloyd, M. E. Umstead, and M. C. Lin, *J. Energ. Mater.* **3**, 187 (1985).
- <sup>57</sup>G. F. Velardez, S. Alavi, and D. L. Thompson, *J. Chem. Phys.* **123**, 074313 (2005).
- <sup>58</sup>C. Capellos, S. Lee, S. Bulusu, and L. Gams, *Advances in Chemical Reaction Dynamics* (D. Reidel, Dordrecht, 1986).
- <sup>59</sup>A. C. Landerville, I. I. Oleynik, and C. T. White, *J. Phys. Chem. A* **113**, 12094 (2009).
- <sup>60</sup>Y. Q. Guo, A. Bhattacharya, and E. R. Bernstein, *J. Chem. Phys.* **128**, 034303 (2008).
- <sup>61</sup>Y. Guo, A. Bhattacharya, and E. R. Bernstein, *J. Chem. Phys.* **134**, 024318 (2011).
- <sup>62</sup>See supplementary material at <http://dx.doi.org/10.1063/1.4752654> for details of calculations and methods.